Crosslinkable Poly(vinyl acetate)/Clay Nanocomposite Films Cast from Soap-Free Emulsion-Polymerized Latices

An-Ting Chien,[1] Yuan-Haun Lee,[2] King-Fu Lin[1,2]

[1]*Institute of Polymer Science and Engineering, National Taiwan University, Taipei, Taiwan, Republic of China*
[2]*Department of Materials Science and Engineering, National Taiwan University, Taipei, Taiwan, Republic of China*

Received 30 August 2007; accepted 26 December 2007
DOI 10.1002/app.28066
Published online 28 March 2008 in Wiley InterScience (www.interscience.wiley.com).

ABSTRACT: Exfoliated poly(vinyl acetate) (PVAc)/montmorillonite (MMT) and poly(vinyl acetate-*co*-glycidyl methacrylate) [P(VAc-*co*-GMA)]/MMT nanocomposite latices, prepared by soap-free emulsion polymerization, were able to be cast into films, and the latter was crosslinked with diethylene triamine as a curing agent. The glass-transition temperature of the crosslinked P(VAc-*co*-GMA)/MMT nanocomposite films was higher than that of the PVAc/MMT counterparts. Although both the Young's modulus and yield stress for the PVAc/MMT nanocomposite films increased with the content of MMT, the extent of the increase was greater for the crosslinked P(VAc-*co*-GMA)/MMT nanocomposites. The exfoliated MMT nanoplatelets retarded the cold drawing of the PVAc matrix during tensile testing, resulting in a decrease of the elongation. However, crosslinked P(VAc-*co*-GMA)/MMT nanocomposite films still had more elongation than the PVAc/MMT counterparts. The drastic decrease of the water vapor permeability with the content of MMT for both types of nanocomposite films suggested that the exfoliated MMT nanoplatelets were dispersed evenly and flattened completely along the film surface. After all the nanocomposite film samples were burned, the inflammable residues for the samples with an MMT content higher than 5 wt % could preserve the original film profile with stiffness, and this indicated that the exfoliated MMT nanoplatelets acted as inflammable scaffolds. © 2008 Wiley Periodicals, Inc. J Appl Polym Sci 109: 355–362, 2008

Key words: latices; nanolayers; nanocomposites

INTRODUCTION

Since nylon 6/montmorillonite (MMT) nanocomposites were invented by a Toyota research group,[1–3] polymer–clay nanocomposites have attracted vast attention because of their superior properties with respect to conventional composite materials.[4–6] A small amount of the clay dispersed in the polymeric matrix can significantly improve the mechanical properties,[7] thermal stability,[8] barrier properties,[9] and ionic conductivities.[10] Various polymers, clays, processes, and characteristics associated with polymer/clay nanocomposites have been reported recently.[11–15] Although researchers have usually adopted certain organic modifications for clay to access exfoliated polymer/clay nanocomposites, Park et al.[16] successfully used soap-free emulsion polymerization to prepare exfoliated poly(methyl methacrylate) (PMMA)/MMT nanocomposites for optical applications without the organic modification of clay to minimize the light scattering loss caused by a surfactant.

Soap-free emulsion polymerization in an aqueous solution is a clean and prevailing process for manufacturing polymer latices.[17–21] Recently, in our laboratory, we have investigated the exfoliation process of MMT during the soap-free emulsion polymerization of methyl methacrylate in the presence of MMT.[22] It was surprising to find that the polymerizing chains were aggregated into a disk form inside the clay interlayer regions for micellation and eventually exfoliated the MMT. The exfoliation of MMT was almost completed in the micellation stage. However, because the as-formed exfoliated PMMA/MMT nanocomposite latex particles are too rigid to form a film by casting, their applications are limited. To solve this problem, poly(vinyl acetate) (PVAc) was employed to replace the PMMA matrix.[23] The cast films from the PVAc/MMT nanocomposite latices were transparent, with the exfoliated MMT nanoplatelets in a flat form uniformly dispersed in the PVAc matrix. As a result, the exfoliated MMT nanoplatelets in the film effectively reduced the water vapor permeability of PVAc.

In this study, to extend the application of PVAc/MMT nanocomposite films, we introduced an extra crosslinkable glycidyl methacrylate (GMA) monomer into soap-free emulsion polymerization. The result-

Correspondence to: K.-F. Lin (kflin@ccms.ntu.edu.tw).
Contract grant sponsor: National Science Council in Taiwan, Republic of China; contract grant number: NSC95-2216-E-002-206.

Journal of Applied Polymer Science, Vol. 109, 355–362 (2008)

ing poly(vinyl acetate-*co*-glycidyl methacrylate) [P(VAc-*co*-GMA)]/MMT nanocomposite latex could be crosslinked with diethylene triamine as a curing agent. Although the Young's modulus and yield stress of the PVAc/MMT nanocomposite films were increased with the content of MMT, those of the crosslinked P(VAc-*co*-GMA)/MMT counterparts were increased more. Besides, the crosslinked P(VAc-*co*-GMA)/MMT nanocomposite films also had more elongation than the PVAc/MMT counterparts. Interestingly, after all the nanocomposite films were burned, the inflammable residues for the samples with an MMT content higher than 5 wt % could preserve their original film profile with stiffness, and this indicated that the exfoliated MMT nanoplatelets acted as inflammable scaffolds.

EXPERIMENTAL

Materials

Vinyl acetate (VAc) and GMA monomers were purchased from Acros (Stuttgart, Germany). Both were distilled under reduced pressure before use to remove an inhibitor. Potassium persulfate (KPS) and diethylene triamine, from Across and Sigma, were directly used as the initiator and curing agent, respectively. MMT (PK-802), with a cationic exchange capacity of 114 mequiv/100 g, was purchased from Pai Kong Nanotechnology (Hsinchu, Taiwan).

Preparation of the PVAc/MMT and P(VAc-*co*-GMA)/MMT nanocomposite latices

To a three-necked flask loaded with 125 mL of deionized water were added 0.3852 g of KPS and an allocated amount of MMT for the preparation of PVAc/MMT nanocomposite latices containing 0, 1, 3, 5, or 10 wt % MMT. After stirring at room temperature for intercalation overnight, 9.5 g of VAc monomer was added for soap-free emulsion polymerization. The solutions were maintained at 50°C for 50 h first and then heated to 70°C for $\sim$ 3 h until no further polymerization was detected. The conversion of polymerization was $\sim$ 80%. The PVAc/MMT nanocomposite latex containing 1 wt % MMT, for example, was designated as the PVAc/1% MMT nanocomposite latex. For the preparation of P(VAc-*co*-GMA)/MMT nanocomposite latices, 9.5 g of mixed VAc and GMA monomers in a molar ratio of 9 : 1 was used with otherwise the same amounts of deionized water, KPS, and MMT in the solution as those for the preparation of PVAc/MMT nanocomposite latices. The solutions were directly heated to 70°C for conducting the soap-free emulsion polymerization. After no further polymerization was detected, a small amount of the latex solution was removed, diluted, and dried to obtain the latex particles for transmission electron microscopy (TEM) observation. The remaining latex solutions were stored in the refrigerator for the next step of film preparation.

Preparation of the PVAc/MMT and crosslinked P(VAc-*co*-GMA)/MMT nanocomposite films

The PVAc/MMT nanocomposite latices, after homogeneous stirring, were poured into a rectangular aluminum-foil mold with dimensions of 15 $\times$ 45 cm^2 and then heated to 50°C in an oven. After 12 h, they were further heated to 70°C to remove the residual water or monomer until a clear PVAc/MMT nanocomposite film $\sim$ 0.15 mm thick was formed. To prepare the crosslinked P(VAc-*co*-GMA)/MMT nanocomposite films, the P(VAc-*co*-GMA)/MMT nanocomposite latices were thoroughly mixed with 0.43 g of the diethylene triamine curing agent before being poured into a similar rectangular aluminum-foil mold and heated to 50°C in an oven. After 12 h, the film was further cured at 100°C for 30 min to afford the crosslinked P(VAc-*co*-GMA)/MMT nanocomposite film.

Characterization

TEM of the specimens was investigated mainly with a JEOL JSM-1230 transmission electron microscope (Japan). X-ray diffraction patterns of the film and powder samples were recorded with a Philip XRD-500 X-ray diffraction analyzer (England) with nickel-filtered Cu Kα radiation at 30 kV and 20 mA. The molecular weights of PVAc and P(VAc-*co*-GMA) matrices removed from their respective nanocomposite latices by Soxhlet extraction[23] were measured by gel permeation chromatography, which was carried out at 40°C with a Testhigh series III pump (England) and a Testhigh model 500 ultraviolet–visible (UV–vis) detector. One Phenol Gel 550A column and two Phenol Gel MXL columns in series were used with tetrahydrofuran as a mobile phase (0.8 mL/min). The molecular weights and molecular weight distributions were estimated by reference to the polystyrene standard.

UV–vis absorption spectra of the film samples were recorded on a Jasco model 555 spectrometer (Japan). Fourier transform infrared (FTIR) spectra of the latex samples were recorded on a Jasco model 470 FTIR instrument. Their thermal degradation behavior was monitored with a PerkinElmer 7 thermogravimetric analyzer (Waltham, MA) at a heating rate of 10°C/min under nitrogen. The glass-transition temperature (T_g) was measured with a PerkinElmer Pyris 6 differential scanning calorimeter at a heating rate of 10°C/min. Tensile properties of the film samples, such as the yield stress, Young's modulus, and elongation, were measured with a HungTa

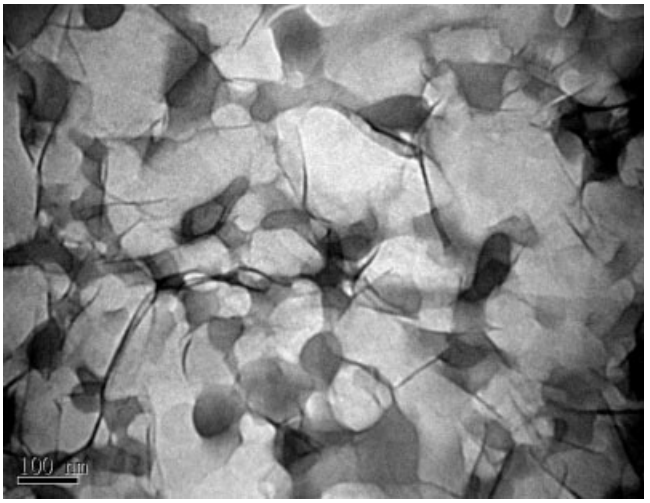

Figure 1 TEM micrograph of the P(VAc-*co*-GMA)/5% MMT nanocomposite latex.

HT-2328 tensile tester (Taiwan) according to ASTM D 638 type IV with a crosshead speed of 1 mm/min at 30°C. At least five specimens were measured for each testing datum. The fracture surface morphology after tensile testing was investigated by scanning electron microscopy (SEM) with a JEOL JSM-6700 high-resolution scanning electron microscope.

The water vapor permeability of the film samples was measured according to ASTM E 96. In general, ~150 mL of deionized water was placed into a cylinder cup. The mouth of the cup was sealed with a film specimen, and the cup was placed on an electronic balance located in an air-conditioned environment. The periodical weight was recorded until the change of the weight with time was linear. The slope of the linear region was used to estimate the water vapor transmission (δ), which was defined as the weight loss per unit of time and unit of area of the film specimen. Then, the permeability coefficient of water vapor (K_V) was estimated with the following equation:

$$K_V = \frac{\delta d}{P_s(1 - R_h)} \quad (1)$$

where d is the thickness of the film specimen, P_s is the saturated water vapor pressure at the testing temperature, and R_h is the relative humidity outside the testing cup expressed as a fraction.

RESULTS AND DISCUSSION

P(VAc-*co*-GMA)/MMT nanocomposite latices

A typical TEM image of the exfoliated P(VAc-*co*-GMA)/MMT nanocomposite latex is shown in Figure 1. Compared to the poorly defined latex particle domains observed for the PVAc/MMT latex,[23] the exfoliated P(VAc-*co*-GMA)/MMT nanocomposite latex showed more discernable domains with a diameter of ~ 100 nm. It has been suggested that because of the hydrophilic nature of PVAc resin, no well-defined PVAc matrix was observed.[23] Thus, GMA units in the resin matrix played a major role in creating the resin domains of ~ 100 nm for the exfoliated P(VAc-*co*-GMA)/MMT nanocomposite latex. The GMA units were also identified by the absorption peak appearing at 925 cm^{-1} in the infrared spectra of the resin matrix, which was contributed by the epoxy groups. As the P(VAc-*co*-GMA)/MMT nanocomposite latex solutions were directly cast into a film, their X-ray diffraction patterns were measured, as presented in Figure 2. The X-ray diffraction pattern of neat MMT particles was also included for comparison. The original interlayer d_{001}-spacing of 1.23 nm at $2\theta = \sim 7^\circ$ of neat MMT disappeared for all the P(VAc-*co*-GMA)/MMT nanocomposite films, and this indicated that MMTs were fully exfoliated and dispersed in the films.

The weight-average molecular weight (M_w) and polydispersity index (PDI) of P(VAc-*co*-GMA) and its resin matrices removed from nanocomposite latices are summarized in Table I. The molecular weight data of PVAc resin matrices from PVAc/MMT nanocomposites are also included for comparison. Basically, M_w of the resin matrix slightly decreased with the content of MMT for both nanocomposite latices. It has been indicated that KPS as an initiator for the preparation of a PVAc/MMT nanocomposite latex is intercalated into the interlayer regions of MMT, so its concentration is higher in that region. Because the micellation usually occurs in the interlayer regions, the radicals on the growing chains should have more chance to be quenched.[23] The molecular weight of the P(VAc-*co*-GMA) resin matrix in the nanocom-

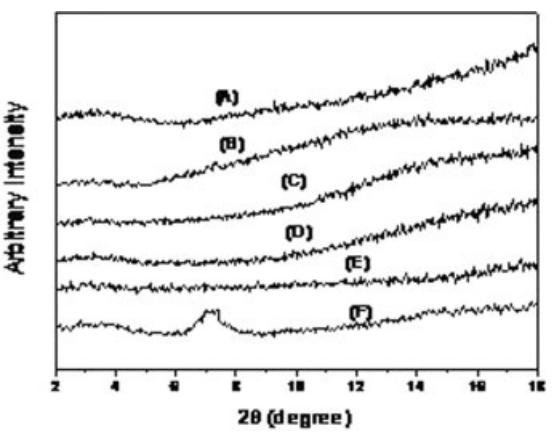

Figure 2 X-ray diffraction patterns of P(VAc-*co*-GMA)/MMT nanocomposite films containing (A) 0, (B) 1, (C) 3, (D) 5, and (E) 10 wt % MMT and (F) pristine MMT particles for comparison.

TABLE I
Properties of the PVAc/MMT and P(VAc-*co*-GMA)/MMT Nanocomposite Films

Sample	$M_w \times 10^5$	PDI	T_g (°C)	T_d (°C)
PVAc	6.45[a]	2.13[a]	30.2	269.4
PVAc/1% MMT	4.40[a]	2.01[a]	34.2	307.8
PVAc/3% MMT	4.99[a]	2.73[a]	35.1	306.6
PVAc/5% MMT	4.74[a]	2.44[a]	38.5	309.6
PVAc/10% MMT	3.52[a]	2.23[a]	41.4	311.4
P(VAc-*co*-GMA)	5.44	2.31	44.7[b]	287.3[b]
P(VAc-*co*-GMA)/1% MMT	3.03	2.21	45.7[b]	289.4[b]
P(VAc-*co*-GMA)/3% MMT	3.72	1.96	45.1[b]	292.0[b]
P(VAc-*co*-GMA)/5% MMT	3.16	2.89	46.1[b]	304.1[b]
P(VAc-*co*-GMA)/10% MMT	2.69	2.02	46.3[b]	313.8[b]

[a] Taken from ref. 23.
[b] The sample was crosslinked.

posites was also slightly lower than that of its PVAc counterpart.

PVAc/MMT and crosslinked P(VAc-*co*-GMA)/MMT nanocomposite films

P(VAc-*co*-GMA)/MMT nanocomposite latices after mixing with the diethylene triamine curing agent were then cast into films. After they were cured, the films were transparent but brown, as presented in Figure 3. The brown color resulted from the reacted amino groups of the diethylene triamine curing agent. However, because of light scattering by the exfoliated MMT, the absorption in the entire UV–vis spectrum was increased with the MMT content, as shown in Figure 4. Because PVAc/MMT nanocomposites have no extra absorption in the visible region, they appear as a transparent and colorless film.[23] However, it is noteworthy that for the crosslinked P(VAc-*co*-GMA)/MMT nanocomposite films, as the MMT content reached 5 wt %, extra absorption in the UV region was so high that they might have potential to be used as UV-screening films.

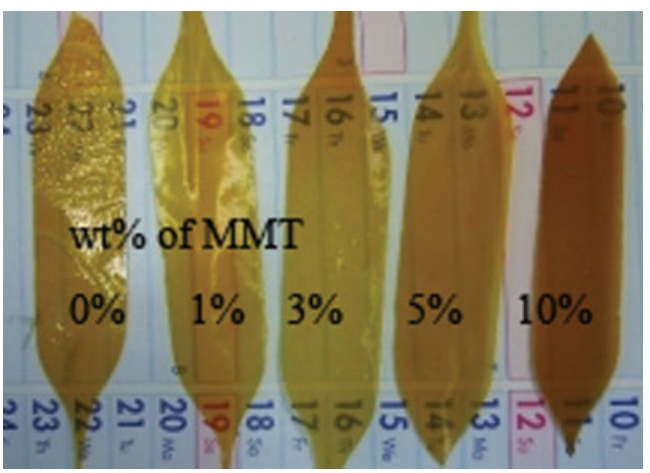

Figure 3 Photographs of crosslinked P(VAc-*co*-GMA)/MMT nanocomposite films with indicated MMT contents. [Color figure can be viewed in the online issue, which is available at www.interscience.wiley.com.]

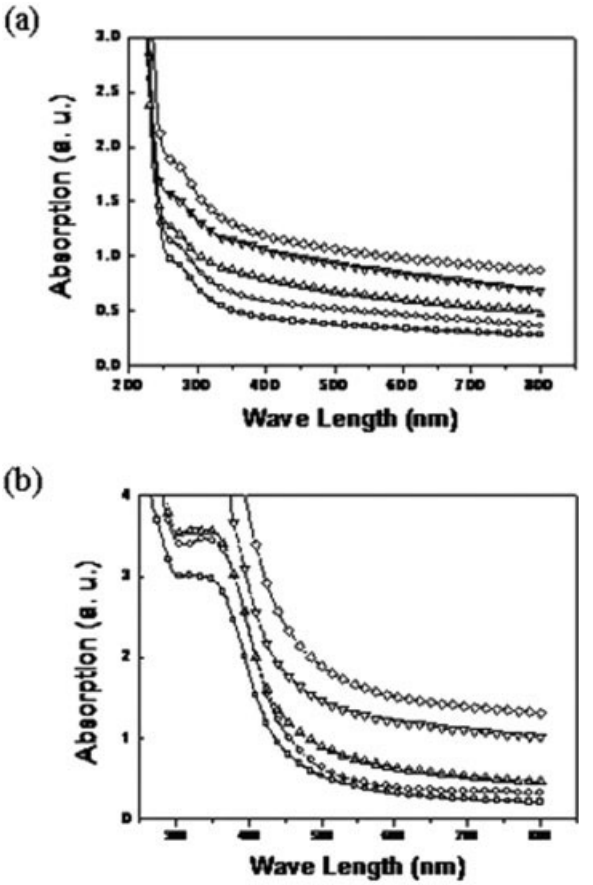

Figure 4 UV–vis absorption spectra of (a) PVAc/MMT and (b) crosslinked P(VAc-*co*-GMA)/MMT nanocomposite films containing (□) 0, (○) 1, (△) 3, (▽) 5, or (◇) 10 wt % MMT.

T_g of the PVAc/MMT nanocomposite films was increased with the MMT content, as illustrated in their differential scanning calorimetry (DSC) thermograms shown in Figure 5(a), and this is consistent with the reported behavior for most of the exfoliated polymer/MMT nanocomposites; that is, the exfoliated MMT nanoplatelets would retard the segmental motion of polymer chains.[6] However, although T_g of the crosslinked P(VAc-*co*-GMA)/MMT nanocomposite films was higher than that of the PVAc/MMT counterparts, it was barely changed with the content of MMT. All the T_g data for the nanocomposite films are summarized in Table I. Exfoliated MMT nanoplatelets can also increase the degradation temperature (T_d) of PVAc/MMT nanocomposite films, as illustrated in their thermogravimetric analysis (TGA) plots shown in Figure 6(a). T_d of the film samples was estimated at the 5% loss of weight in the TGA plots and is also summarized in Table I. As shown in the table, incorporating 1 wt % MMT could raise T_d from 269.4 to 307.8°C. However, a further increase

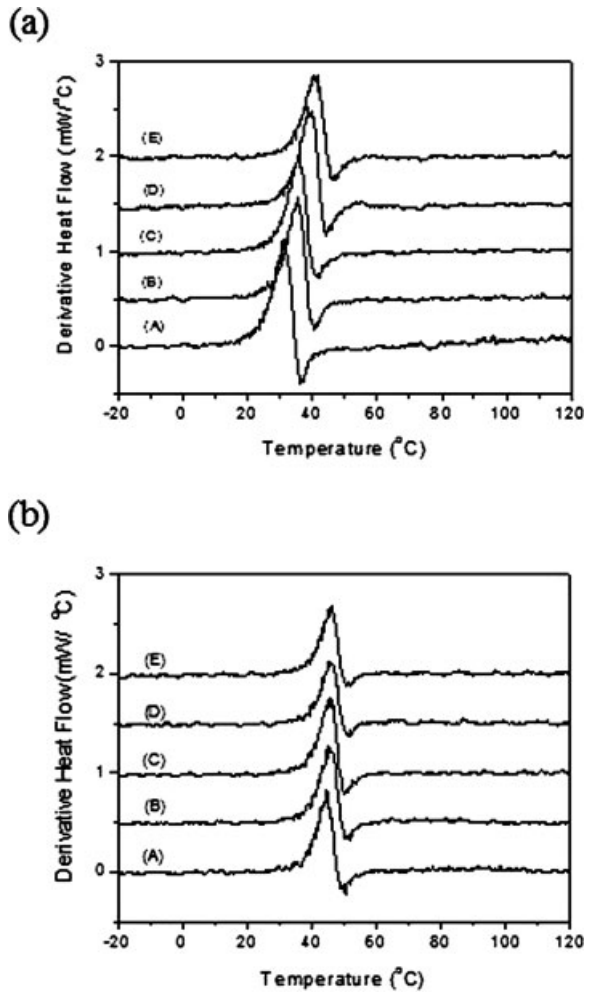

Figure 5 Derivative DSC thermograms of (a) PVAc/MMT and (b) crosslinked P(VAc-*co*-GMA)/MMT nanocomposite films containing (A) 0, (B) 1, (C) 3, (D) 5, or (E) 10 wt % MMT.

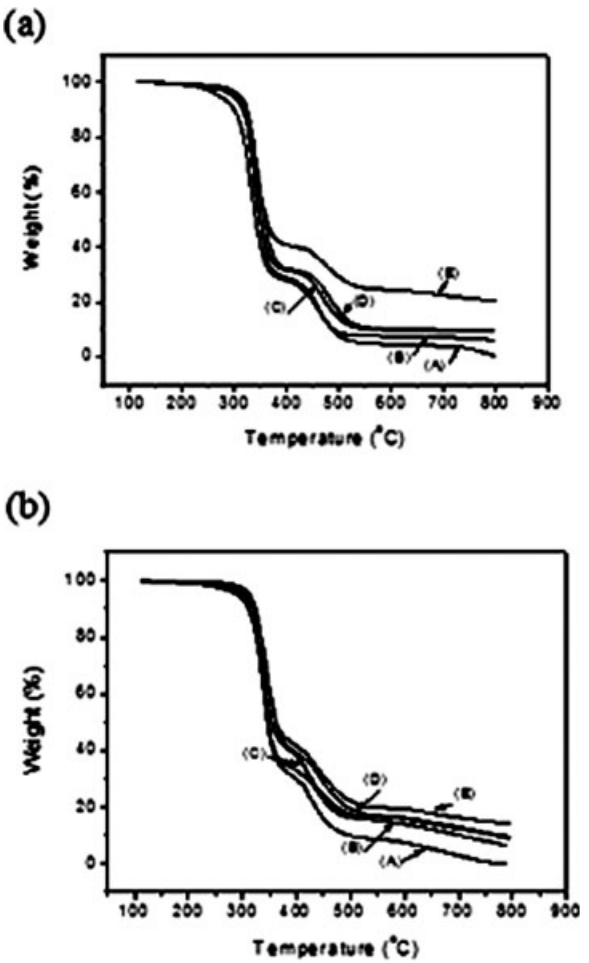

Figure 6 TGA plots of (a) PVAc–MMT and (b) crosslinked P(VAc-*co*-GMA)/MMT nanocomposite films containing (A) 0, (B) 1, (C) 3, (D) 5, or (E) 10 wt % MMT.

in the MMT content only slightly increased T_d. For the crosslinked P(VAc-*co*-GMA)/MMT nanocomposite films, although T_d was only slightly increased with the content of MMT, incorporating 1 wt % MMT indeed increased the char yield [see Figs. 6(b)].

The P(VAc-*co*-GMA)/MMT and crosslinked P(VAc-*co*-GMA)/MMT nanocomposite films were then subjected to burning with fire, and their inflammable residues are illustrated in Figure 7. Neat PVAc and crosslinked P(VAc-*co*-GMA) films were immediately burned into black ash as soon as they were brought close to the flame. However, the films containing MMT had a retarded burning speed. When the MMT content was higher than 5 wt %, the inflammable residue even preserved the original film profile with stiffness. Because the MMT nanoplatelets were dispersed evenly and flattened almost completely along the film surface,[23] they acted like scaffolds to preserve the film profile after burning. It is noteworthy that once combustion occurs, this scaffold would have the potential to block flame transportation.

Figure 8 shows the tensile properties of PVAc/MMT and crosslinked P(VAc-*co*-GMA)/MMT nanocomposite films, such as the Young's modulus, yield

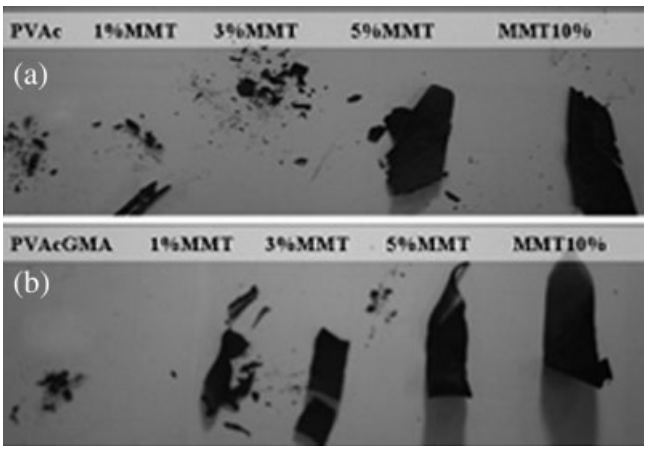

Figure 7 Photographs of burned residues of (a) PVAc/MMT and (b) crosslinked P(VAc-*co*-GMA)/MMT nanocomposite films with indicated contents of MMT.

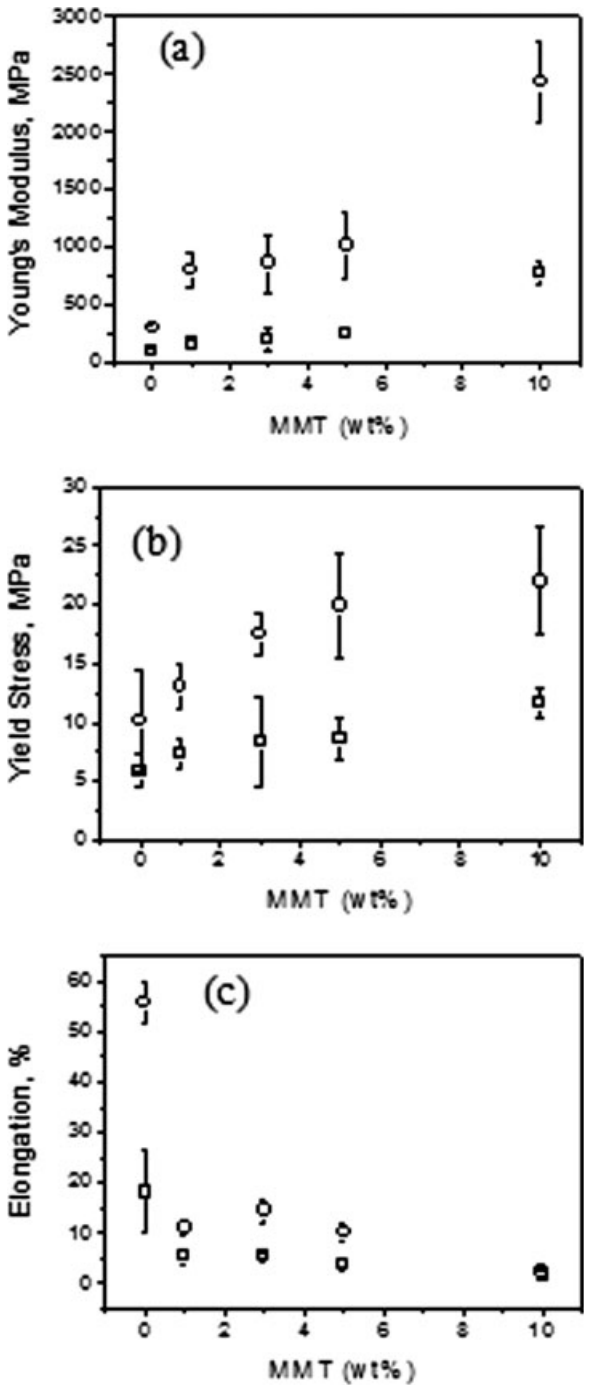

Figure 8 (a) Young's modulus, (b) yield stress, and (c) elongation of (□) PVAc/MMT and (○) crosslinked P(VAc-*co*-GMA)/MMT nanocomposite films as a function of the MMT content.

stress, and elongation, as a function of the MMT content. Although the Young's modulus and yield stress increased with the content of MMT for both nanocomposite films, crosslinked P(VAc-*co*-GMA)/MMT nanocomposite films had much higher Young's modulus, yield stress, and even elongation than the PVAc/MMT counterparts. As the content of MMT reached 5 wt %, both the Young's modulus and yield strength of the crosslinked P(VAc-*co*-GMA)/MMT nanocomposites were almost double those of the crosslinked P(VAc-*co*-GMA) films. However, elongation was significantly decreased when exfoliated MMT nanoplatelets (1 wt %) were incorporated into both PVAc/MMT and crosslinked P(VAc-*co*-GMA)/MMT films. This was due to the fact that cold drawing of the polymer chains[24] during tensile testing was retarded by the incorporated MMT nanoplatelets, as illustrated in Figure 9(a), which shows only small, striplike ductile resins protruding from the fracture surface of the PVAc/1% MMT film. For the PVAc/10% MMT film, cold drawing was completely prohibited, as shown in Figure 9(b).

Figure 10 shows the water vapor permeability coefficients of PVAc/MMT and crosslinked P(VAc-*co*-GMA)/MMT nanocomposite films as a function of the MMT content. The water vapor permeability

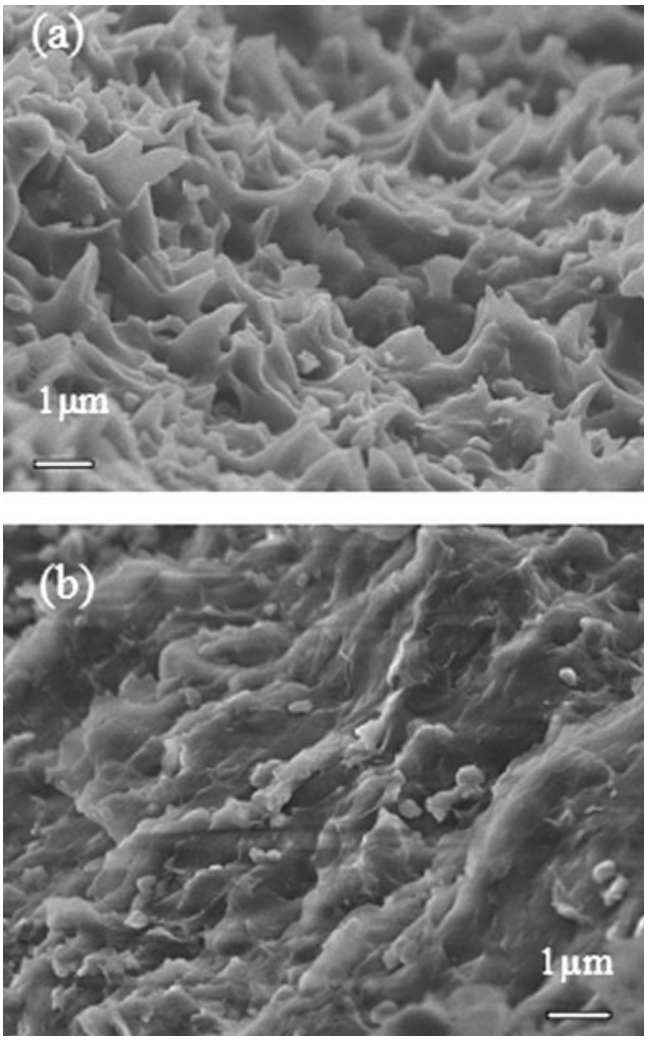

Figure 9 SEM micrographs of the fracture surfaces of tensile specimens for the PVAc/MMT nanocomposite films containing (a) 1 or (b) 10 wt % MMT.

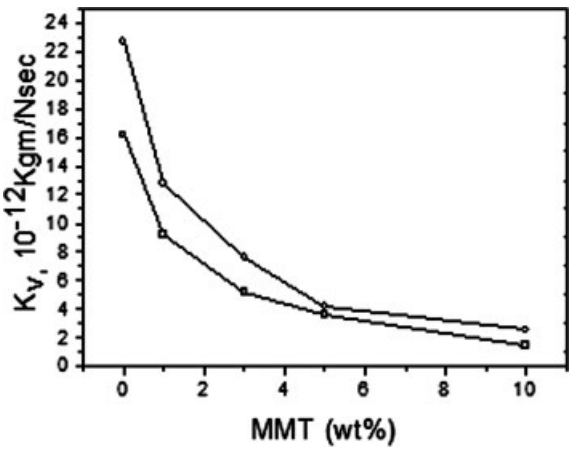

Figure 10 Water vapor permeability coefficient (K_V) values of (□) PVAc/MMT and (○) crosslinked P(VAc-*co*-GMA)/MMT nanocomposite films as a function of the MMT content.

coefficients for both PVAc and crosslinked P(VAc-*co*-GMA) films were significantly reduced by the incorporation of MMT nanoplatelets because the vapor could not penetrate the MMT nanoplatelets. For the PVAc/MMT nanocomposite films, in our previous study, we used the generalized Nielsen permeability model[25,26] to estimate the average aspect ratio of exfoliated MMT platelets and obtained a value of 327, which is similar to those directly estimated by atomic force microscopy and TEM.[23] Accordingly, it was suggested that the MMTs in the PVAc/MMT nanocomposite films were fully exfoliated, dispersed evenly, and flattened completely along the film surface. Although the cured P(VAc-*co*-GMA)/MMT nanocomposite films had slightly higher water vapor permeability coefficients than their PVAc/MMT counterparts, the average aspect ratio of their exfoliated MMT platelets calculated from the generalized Nielsen permeability model was 320. The difference in the aspect ratio between PVAc/MMT and crosslinked P(VAc-*co*-GMA)/MMT nanocomposite films was within the experimental error. Apparently, the MMTs in the cured P(VAc-*co*-GMA)/MMT nanocomposite films were also fully exfoliated, dispersed evenly, and flattened completely along the film surface. The slightly higher water vapor permeability for crosslinked P(VAc-*co*-GMA)/MMT nanocomposite films compared to their PVAc/MMT counterparts might be due to the curing phenomenon. It has been reported that crosslinking tends to reduce the density of the resin, leading to an increase in the free volume.[27]

Although the crosslinked P(VAc-*co*-GMA)/MMT nanocomposite films have a slightly higher water vapor permeability, they are more durable than their PVAc/MMT counterparts and have superior mechanical properties. Their fabrication is facile, and their applications are versatile. Their potential applications for coatings, painting, adhesives, sealing materials, and so forth are currently under investigation.

CONCLUSIONS

PVAc/MMT and crosslinked P(VAc-*co*-GMA)/MMT nanocomposite films were successfully fabricated via soap-free emulsion polymerization. The exfoliated MMT nanoplatelets were dispersed evenly and flattened completely along the film surface. For the nanocomposite films with an MMT content higher than 5 wt %, the exfoliated MMT nanoplatelets could perform as inflammable scaffolds during combustion. Although the Young's modulus and yield stress of the PVAc/MMT nanocomposite films were increased with the content of MMT, crosslinking of the P(VAc-*co*-GMA)/MMT nanocomposite films could enhance this effect. Besides, crosslinked P(VAc-*co*-GMA)/MMT nanocomposite films have higher T_g and more elongation than their PVAc/MMT counterparts. We believe that those superior properties of the crosslinkable P(VAc-*co*-GMA)/MMT nanocomposite latices and films can justify their potential applications for coatings, adhesives, sealing materials, and so forth.

References

1. Kojima, Y.; Usuki, A.; Kawasumi, M.; Okada, A.; Kurauchi, T.; Kamigaito, O. J Polym Sci Part A: Polym Chem 1993, 31, 983.
2. Usuki, A.; Kojima, Y.; Kawasumi, M.; Okada, A.; Fukushima, Y.; Kurauchi, T.; Kamigaito, O. J Mater Res 1993, 8, 1179.
3. Kojima, Y.; Usuki, A.; Kawasumi, M.; Okada, A.; Kurauchi, T.; Kamigaito, O. J Polym Sci Part A: Polym Chem 1993, 31, 1755.
4. Pinnavaia, T. J.; Beall, G. E. Polymer–Clay Nanocomposites; New York: Wiley, 2000.
5. Utracki, L. A. Clay-Containing Polymeric Nanocomposites; Rapra Technology: Shrewsbury, England, 2004.
6. Ke, Y. C.; Stroeve, P. Polymer-Layered Silicate and Silica Nanocomposites; Elsevier: Amsterdam, 2005.
7. Haraguchi, K.; Ebato, M.; Takehisa, T. Adv Mater 2006, 18, 2250.
8. Ma, J.; Yu, Z. Z.; Zhang, Q. X.; Xie, X. L.; Mai, Y. W.; Luck, I. Chem Mater 2004, 16, 757.
9. Yano, K.; Usuki, A.; Okada, A. J Polym Sci Part A: Polym Chem 1997, 35, 2289.
10. Tu, C. W.; Liu, K. Y.; Chien, A. T.; Yen, M. H.; Weng, T. H.; Ho, K. C.; Lin, K. F. J Polym Sci Part A: Polym Chem 2008, 46, 47.
11. Fornes, T. D.; Hunter, D. L.; Paul, D. R. Macromolecules 2004, 37, 1793.
12. Tsai, T. Y.; Li, C. H.; Chang, C. H.; Cheng, W. H.; Hwang, C. L.; Wu, R. J. Adv Mater 2005, 17, 1769.
13. Fan, X. W.; Xia, C. J.; Advincula, R. C. Langmuir 2005, 21, 2537.
14. Lin, K. F.; Hsu, C. Y.; Huang, T. S.; Chiu, W. Y.; Lee, Y. H.; Young, T. H. J Appl Polym Sci 2005, 98, 2042.
15. Zhao, Q.; Samulski, E. T. Macromolecules 2005, 38, 7967.
16. Yeom, E. H.; Kim, W. N.; Kim, J. K.; Lee, S. S.; Park, M. Mol Cryst Liq Cryst 2004, 425, 85.

17. Song, S.; Poehlein, G. W. J Colloid Interface Sci 1989, 128, 486.
18. Hansen, F. K.; Ugelstad, J. J Polym Sci Part A: Polym Chem 1978, 16, 1953.
19. Chen, Y. C.; Lee, C. F.; Chiu, W. Y. J Appl Polym Sci 1996, 61, 2235.
20. Lin, K. F.; Shieh, Y. D. J Appl Polym Sci 1998, 69, 2069.
21. Lin, K. F.; Shieh, Y. D. J Appl Polym Sci 1998, 70, 2313.
22. Lin, K. F.; Lin, S. C.; Chien, A. T.; Hsieh, C. C.; Yen, M. H.; Lin, C. S.; Chiu, W. Y.; Lee, Y. H. J Polym Sci Part A: Polym Chem 2006, 44, 5572.
23. Chien, A. T.; Lin, K. F. J Polym Sci Part A: Polym Chem 2007, 45, 5583.
24. Nielsen, L. E. Mechanical Properties of Polymers and Composites; Marcel Dekker: New York, 1974; Vol. 2.
25. Bharadwaj, R. K. Macromolecules 2001, 34, 9189.
26. Nielsen, L. E. J Macromol Sci Chem 1967, 1, 929.
27. Kong, E. S. In Characterization of Highly Cross-linked Polymers; Labana, S. S.; Dickie, R. A., Eds.; ACS Symposium Series 243; American Chemical Society: Washington DC, 1984; Chapter 9.